HHS Public Access

Author manuscript

Eur J Neurosci. Author manuscript; available in PMC 2016 February 16.

Published in final edited form as:

Eur J Neurosci. 2016 January ; 43(2): 148–161. doi:10.1111/ejn.13081.

Thyroid hormone is required for pruning, functioning and long-term maintenance of afferent inner hair cell synapses

Srividya Sundaresan[1], **Jee-Hyun Kong**[1], **Qing Fang**[2], **Felipe T. Salles**[1], **Felix Wangsawihardja**[1], **Anthony J. Ricci**[1], and **Mirna Mustapha**[1]

[1] Department of Otolaryngology-Head & Neck Surgery, Stanford University, 300 Pasteur Drive, Room R111A, Stanford, CA 94035, USA

[2] Department of Human Genetics, University of Michigan, Ann Arbor, MI, USA

Abstract

Functional maturation of afferent synaptic connections to inner hair cells (IHCs) involves pruning of excess synapses formed during development, as well as the strengthening and survival of the retained synapses. These events take place during the thyroid hormone (TH)-critical period of cochlear development, which is in the perinatal period for mice and in the third trimester for humans. Here, we used the hypothyroid Snell dwarf mouse (*Pit1*^{dw}) as a model to study the role of TH in afferent type I synaptic refinement and functional maturation. We observed defects in afferent synaptic pruning and delays in calcium channel clustering in the IHCs of *Pit1*^{dw} mice. Nevertheless, calcium currents and capacitance reached near normal levels in *Pit1*^{dw} IHCs by the age of onset of hearing, despite the excess number of retained synapses. We restored normal synaptic pruning in *Pit1*^{dw} IHCs by supplementing with TH from postnatal day (P)3 to P8, establishing this window as being critical for TH action on this process. Afferent terminals of older *Pit1*^{dw} IHCs showed evidence of excitotoxic damage accompanied by a concomitant reduction in the levels of the glial glutamate transporter, GLAST. Our results indicate that a lack of TH during a critical period of inner ear development causes defects in pruning and long-term homeostatic maintenance of afferent synapses.

Keywords

auditory system; calcium current; capacitance measurements; glutamate transporter

Introduction

Early neuronal development is marked by overabundant outgrowth of axons and dendrites that innervate multiple targets. Inappropriate or excess neuronal connections are subsequently pruned back, resulting in a mature neuronal circuit. Defective or abnormal neuronal pruning can result in various neurological and behavioural disorders (Paolicelli *et al*., 2011; Zhan *et al*., 2014). Cochlear afferent innervation also undergoes pruning as the organ of Corti matures into a fully functioning organ (Sobkowicz *et al*., 1982; Huang *et al*.,

Correspondence: Dr Mirna Mustapha, as above. mirnam@stanford.edu.

2012). However, the mechanisms regulating the postnatal events that lead to a mature pattern of afferent innervation in the cochlea are not well understood. It is well known that thyroid hormone (TH) is required for normal development of both the central and peripheral nervous systems in a temporally sensitive manner (Bernal, 2005). Previous studies have shown that hypothyroidism alters neuronal connectivity to inner hair cells (IHCs) and outer hair cells, impairs their function, disrupts synaptic pruning, and alters vesicle release (Uziel *et al*., 1983; Rusch *et al*., 2001; Rueda *et al*., 2003; Brandt *et al*., 2007; Sendin *et al*., 2007), indicating an important role of TH action on these processes. These studies also raised several interesting questions regarding the mechanisms that control the retraction of excess neurites and the strengthening and survival of the retained connections such as: (i) what are the quantitative effects of hypothyroidism on presynaptic and postsynaptic pruning; (ii) are the excess synapses in hypothyroid IHCs functionally mature; (iii) what is the developmental time window for TH action on synaptic pruning; and (iv) does disrupted synaptic pruning resulting from hypothyroidism have long-term effects on synaptic maintenance? Addressing these questions will allow us to gain insights into the mechanisms regulating the pruning and survival of afferent IHC synapses in the cochlea, and reveal the functional consequences of these mechanisms being disrupted.

In this study, we used the Snell dwarf (*Pit1*^{dw}, officially *Pou1f1*^{dw}) hypothyroid mouse (Karolyi *et al*., 2007; Mustapha *et al*., 2009) model to address the questions outlined above focusing on IHC afferent synapses. We quantified the number of synapses under hypothyroid conditions at different time points during the postnatal period of the TH-critical window for cochlear development, which extends from embryonic day 18 to postnatal day (P)12 (Deol, 1973; Uziel, 1986; Knipper *et al*., 1999). We determined the functional status of the afferent synapses in the *Pit1*^{dw} IHCs by analysing the recruitment of calcium channels to the synapses and by measuring calcium current and membrane capacitance. To determine the effect of hypothyroidism on the long-term maintenance of afferent IHC synapses, we examined the synaptic structure in older (P42) mice. We also determined the critical window for TH action on synaptic pruning by carrying out TH replacement for finite periods in the *Pit1*^{dw} mice. Our results provide several novel insights into the structure and function of afferent synapses in hypothyroid conditions, the effect of TH on long-term synaptic maintenance, and the critical window required for TH action on synaptic pruning.

Materials and methods

Mice

DW/J *Mlph*^{ln} *Pit*^{dw}/J mice were obtained from the Jackson Laboratory in 1990, and are maintained at Stanford University. Established procedures for animal care and genotyping were used, including feeding the mice a higher-fat chow designed for breeding (PMI5020), delayed weaning of mutants at P35, and housing mutants with normal littermates to provide warmth (Karolyi *et al*., 2007). P0 is the day of birth. All experiments were approved by the University Committee on the Use and Care of Animals, and conducted in accord with the principles and procedures outlined in the National Institutes of Health Guidelines for the Care and Use of Experimental Animals.

Immunofluorescence staining and confocal microscopy

RIBEYE and SHANK1 were used as presynaptic and postsynaptic markers, respectively. Another marker, CaV1.3, identified this calcium channel at the synapse. Inner ears were dissected into cold phosphate-buffered saline (PBS), and, after opening of the oval and round windows and the bone at the cochlear apex, cochleas were perfused with 4% paraformaldehyde in PBS and left in fixative solution for an additional 10 min. Samples were washed in PBS for 10 min, and then blocked in PBS containing 0.5% Triton X-100 and 5% bovine serum albumin for 30 min at room temperature. The same blocking buffer was used for diluting antibodies. Primary antibodies were incubated at 4 °C for 36 h, and this was followed by three washes in PBS with 0.1% Tween. Secondary antibodies were added for 1 h at room temperature, and this was followed by three washes in PBS with 0.1% Tween. The following polyclonal primary antibodies were used: goat anti-CtBP2 (1 : 200; Santa Cruz Biotechnology) for RIBEYE, rabbit anti-SHANK1 (1 : 200; Neuromics), rabbit anti-CaV1.3 (1 : 500; Alomone), goat anti-GLAST (1 : 200; Cell Signaling), and rabbit anti-myosin VIIa (1 : 300; Proteus Biosciences). The secondary antibodies used were Alexa Fluor 488-conjugated anti-goat and Alexa Fluor 546-conjugated anti-rabbit (1 : 500; Invitrogen). Subsequently, the cochleas were decalcified in 10% EDTA for 1 h at room temperature, and further fixed by immersion in 4% paraformaldehyde in PBS for 15 min. Cochleas were washed in PBS and mounted on slides in ProLong (Invitrogen) anti-fading medium. Confocal images of cochlear whole mount preparations were reconstructed in *z*-stacks with VOLOCITY 3D IMAGE ANALYSIS software to count the numbers of synaptic puncta. The data shown are from the mid-turn of the cochlea.

Quantification and statistical analysis

Quantification of RIBEYE, SHANK1, CaV1.3 and co-localized RIBEYE and SHANK1 (representing a ‘synapse’) or CaV1.3 puncta was performed as previously described (Mendus *et al*., 2014). A minimum of 10 IHCs per mouse and four to seven mice per genotype or treatment group were used for each marker. Marker counts are shown as box and whisker plots that represent every data point in the set. The whiskers represent the minimum and maximum values in the specific group examined. Outliers in the data set are also shown. Statistical analyses were performed with ANOVA [SPSS STATISTICS PREMIUM GRAD PACK (IBM), or MATLAB (Mathworks, Natick, MA, USA)]. Two-way ANOVA of the immunoh istochemistry data was performed with synaptic marker counts as the dependent variable, and with genotype (wild type or *Pit1*^{Dw}) and treatment or age as independent factors for these tests. On the basis of significant main effects and interactions from this statistical test, planned comparisons were performed by the use of Student’s *t*-test or a one-way ANOVA with marker count as the dependent variable, followed by Scheffe’s *post hoc* test to identify differences between genotypes, or across ages or treatment groups (SPSS and MICROSOFT EXCEL). In all statistical tests, a *P*-value of <0.05 was considered to be statistically significant.

Cochlear RNA extraction and quantitative RT-PCR

Cochleas were dissected, and RNA extraction and cDNA preparation were performed as previously described (Mendus *et al*., 2014). To quantify mRNA expression levels, the cDNA was amplified in Taqman PCR assays (Applied Biosystems, Foster City, CA, USA).

We used proprietary probes and primers from Applied Biosystems for *CaV1.3* (assay ID Mm01209919_m1), *GLAST* (assay ID Mm00600697_m1), and the glyceraldehyde-3-phosphate dehydrogenase gene (assay ID Mm99999915_g1). All Taqman quantitative PCR assays were performed on a Bio-Rad CFX96 Real-Time System (Bio-Rad, Hercules, CA, USA) with accompanying software for data analysis. Expression of the gene of interest was normalized with respect to the internal standard, the glyceraldehyde-3-phosphate dehydrogenase gene. RNA for each genotype was prepared by pooling RNA from three or four mice. At least four such independent experiments with all samples in triplicate were performed. Statistical analyses were performed with Student's *t*-test on MICROSOFT EXCEL (Microsoft, Redmond, WA, USA).

Calcium current and capacitance measurements

Mice of different ages were decapitated, and cochleas were removed as previously described (Peng *et al*., 2013). Organs of Corti were dissected in a solution containing 140 mM NaCl, 2 mM KCl, 2 mM $CaCl_2$, 2 mM $MgCl_2$, 10 mM HEPES, 6 mM glucose, 2 mM pyruvate, and 2 mM creatine (pH 7.4 and 300-310 mOsm). The tectorial membrane was removed, and the midturn of the organ of Corti was mounted in a recording chamber with single strands of dental floss. The bath was perfused at rates of 0.4-0.5 mL/min and maintained at 20-23 °C. Whole cell patch-clamp was achieved on IHCs from the middle to apical cochlear turns with an Axon 200B amplifier (Molecular Devices) and thick-walled borosilicate patch pipettes (<4 MΩ). Pipettes were filled with an intracellular solution containing 125 mM CsCl, 3.5 mM $MgCl_2$, 5mM ATP, 5 mM creatine phosphate, 10 mM HEPES, 1 mM caesium BAPTA, and 2 mM ascorbate (pH 7.2, 280–290 mOsm). Data were collected by use of an IOTech A/D (DAQ3000) with JCLAMP software (SciSoft) at a rate of 30 kHz, and filtered at 10 kHz. Capacitance was tracked with the dual sinusoidal approach (Schnee *et al*., 2011). This is a fast Fourier transfer-based method (Santos-Sacchi, 2004; Santos-Sacchi *et al*., 1998), and is based on a component solution of a simple model for a patched cell. Two voltage frequencies, *f*1 and *f*2, were summed, and the real and imaginary outputs of the current were used to determine the model components. We used an *f*1 frequency of 3125 Hz. Data were quantified and figures were generated with MICROSOFT EXCEL, MICROCAL ORIGIN, and ADOBE ILLUSTRATOR.

TH injection

Pit1^{dw} mice and control wild-type (WT) mice were subcutaneously injected daily from P3 to P8 with either 20 ng 3,3,5-triiodo-L-thyronine sodium salt (T3) solution/g body weight or PBS as a negative control. T3 solution (20 ng/μL) was prepared by dissolving 1 mg of T3 (Sigma Aldrich, St Louis, MO, USA) in 1 mL of 1 M NaOH and 49 mL of PBS. Radioimmunoassay was used to confirm that this dose of T3 was sufficient to induce normal TH levels in *Pit1*^{dw} mice. Other groups have shown that replacement with T3 rather than T4 (thyroxine) is more effective, becauseit bypasses the necessary conversion of T4 to the more active T3 *in vivo* (Weiss *et al*., 1998; Sui *et al*., 2006). Mice were killed at P14.

Transmission electron microscopy

Transmission electron microscopy (TEM) analyses were performed as previously described (Mustapha *et al*., 2009). Briefly, mice were anaesthetized and fixed with an intracardiac

perfusion of 2.5% glutaraldehyde in 0.15 M cacodylate buffer (pH 7.2) with 0.1% tannic acid. Inner ears were removed and further fixed in the same solution for 2 h. The ears were then decalcified with 3% EDTA with 0.25% glutaraldehyde for 1 week at 4 °C. They were then postfixed in 1% osmium tetraoxide, dehydrated with increasing ethanol concentrations, and embedded in Embed 812 epoxy resin. Embedded ears were sectioned, stained with uranyl acetate and lead citrate, and examined on a Phillips CM-100 transmission electron microscope. A minimum of four mice per group were examined.

Results

Elimination of excess presynaptic and postsynaptic structures formed during development is disrupted in hypothyroid IHCs

In mice, the development of IHC afferent innervation normally starts as early as embryonic day 16, and continues through birth until the onset of hearing at P12 (Ehret, 1976). The pruning of excessive type I afferent neurite branches and synapses formed during development at IHCs is an important aspect of this maturation process (Huang *et al*., 2007, 2012). We examined the IHC synapses in control WT and *Pit1*^{dw} mice by immunohistochemistry with the presynaptic ribbon marker RIBEYE and the postsynaptic markers SHANK1 and GLUTR2/3 at P5, P9, and P14. The results of quantification of both SHANK1 and GLUT2/3 puncta were similar. However, we found that the anti-SHANK1 antibody gave us more consistent results. Therefore, we used SHANK1 data for all subsequent analyses. We analysed both the apical turn and mid-turn of the cochlea. As the results from both cochlear regions were similar, images and quantitative analyses from the mid-turn are shown henceforth. Representative images of immunohistochemistry for RIBEYE and SHANK1 are shown in Fig. 1a–d for P5 and P14 in both WT and *Pit1*^{dw}mice. We quantified puncta that were RIBEYE-positive only, puncta that were SHANK1-positive only, and puncta in which both markers were co-localized (henceforth referred to as RIBEYE–SHANK1). For statistical analysis, two-way ANOVAs were performed with RIBEYE, SHANK1 or RIBEYE– SHANK1 count as the dependent variable, and with genotype (WT or *Pit1*^{dw}) and age (P5, P9, and P14) as independent factors. This analysis showed a significant main effect of genotype × age interaction for all three markers ($F_{2,24}$ = 35.640, P = 0.014 for RIBEYE; $F_{2,24}$ = 314.714, P = 2.2E-5 for SHANK1; $F_{2,24}$ = 55.326, P = 0.002 for RIBEYE–SHANK1). Planned comparisons were performed with a one-way ANOVA, with a specific marker count (RIBEYE, SHANK1, or RIBEYE–SHANK1) as the dependent variable and either age or genotype as the independent factor, as indicated below. This analysis was followed by Scheffe's post hoc test to identify differences between genotypes or across the ages tested.

WT IHCs showed a normal pattern of synaptic pruning (Sobkowicz *et al*., 1982; Huang *et al*., 2012) (Fig. 1a, c and e). Actual counts for marker puncta per IHC are shown in Fig. 1e–i. A one-way ANOVA with RIBEYE count as the variable and age as the independent factor was significant ($F_{2,12}$ = 65.544; P = 3E-6). Scheffe's *post hoc* test showed that the number of RIBEYE puncta was significantly lower at P9 (34%) and at P14 (47%) than at P5 (P = 3.2E-5 for P9 vs. P5; P = 3.7E-7 for P14 vs. P5) (Fig. 1e and g). Similar one-way ANOVAs for SHANK1 and RIBEYE–SHANK1 counts were also significant ($F_{2,12}$ = 62.291 and P =

0.001 for SHANK1; $F_{2,12}$ = 38.430 and P = 3E-5 for RIBEYE–SHANK1). SHANK1 counts were markedly reduced at P9 (52%) and at P14 (57%) as compared with P5 (P = 7E-6 for P9 vs. P5; P = 7.3E-7 for P14 vs. P5; Scheffe's *post hoc* test) (Fig. 1e and h). RIBEYE–SHANK1 puncta counts were also significantly lower at P9 (33%), and at P14 (43%) than at P5 in WT mice (P = 0.0003 for P9 vs. P5; P = 7E-6 for P14 vs. P5; Scheffe's *post hoc* test) (Fig. 1e and i). These results are consistent with a normal pattern of both presynaptic and postsynaptic pruning and elimination of excess synapses in these mice during development. In comparison, age-matched *Pit1*^{dw} IHCs showed reduced pruning in the mid-turn (Fig. 1b, d and f). A one-way ANOVA for RIBEYE counts in these mice was performed ($F_{2,12}$ = 12.616, P = 0.001). *Pit*^{dw} IHCs showed a smaller reduction in RIBEYE counts at P9 (13%, P = 0.032; Scheffe's *post hoc* test) and P14 (21%, P = 0.001; Scheffe's *post hoc* test) than at P5. In contrast, there were no significant changes in SHANK1 and RIBEYE–SHANK1 puncta in *Pit1*^{dw} mice across the ages tested by one-way ANOVA (P = 0.048 for SHANK1; P = 0.121 for RIBEYE–SHANK1). This result implied that, although a normal rate of synapse elimination was not observed in the *Pit1*^{dw} IHCs, pruning had occurred to some extent by P14 only on the presynaptic side.

We found that, at all ages examined, *Pit1*^{dw} IHCs showed a distinctly different synaptic staining pattern from those in WT mice of the same age. At P5, RIBEYE counts were slightly (P = 0.028; Scheffe's *post hoc* test following a one-way ANOVA) lower in WT mice than in *Pit1*^{dw} mice, but SHANK1 and RIBEYE–SHANK1 puncta counts were similar in both genotypes (Fig. 1a, b, g, h and i), suggesting that presynaptic pruning was already underway in WT mice by P5. Moving further along the refinement window at P9 and P14, we found that all three markers were significantly lower in WT than in *Pit*^{dw} mice (RIBEYE, P = 0.025 at P5, P = 0.0001 at P9, and P = 0.0002 at P14; SHANK1, P = 0.0001 at P9 and P = 2E-6 at P14; RIBEYE–SHANK1, P = 0.002 at P9 and P = 0.001 at P14; Scheffe's *post hoc* test following a one-way ANOVA) (Fig. 1g–i). Taken together, these data indicated that pruning of excess afferent synapses failed in the hypothyroid cochlea.

We also found an abnormal pattern of afferent synapses in adult *Pit1*^{dw} IHCs by ultrastructural analysis with TEM. *Pit1*^{dw} IHCs showed a large immature synaptic zone with multiple ribbons, as compared with a single ribbon in WT IHCs, as previously described (Sendin *et al*., 2007) (data not shown). To determine whether the defective pruning of synapses in the hypothyroid IHCs correlated with functional alterations, we examined the composition and function of the IHC afferent synapses in these mice.

Composition and function of IHC afferent presynaptic proteins in *Pit1*^{dw} mice

Calcium channel expression and current measurements in Pit^{dw} and WT IHCs

—In order to determine the percentage of RIBEYE–SHANK1 or co-localized puncta that were functional, we examined the expression and distribution of the calcium channel, CaV1.3. CaV1.3 is the primary calcium channel of both mature and immature IHCs (Engel *et al*., 2002; Brandt *et al*., 2003, 2005; Michna *et al*., 2003). We examined whether there was any alteration in the level of gene expression and distribution of this protein in Pit1^{dw} mice vs. control mice. The mRNA expression levels of CaV1.3 in the organ of Corti at both P4 and P7 were not significantly different between *Pit1*^{dw} and WT cochlea as determined by

quantitative PCR (data not shown). We investigated the expression pattern and presynaptic distribution of the CaV1.3 protein by using immunohistochemistry with anti-CaV1.3 and anti-RIBEYE antibodies at P7, P14, and P24, followed by confocal imaging and counting of labelled puncta (Fig. 2a–f). We then performed a two-way ANOVA with marker count as the dependent variable and age and genotype as independent factors. This analysis showed a significant genotype × age interaction ($F_{2,28}$ = 8.157, P = 0.002 for RIBEYE; $F_{2,28}$ = 75.039,P = 5.6E-12forCaV1.3;and$F_{2,28}$ = 5.440, P = 3.1E5 for co-localized RIBEYE and CaV1.3). This analysis was followed by one-way ANOVA for planned comparisons between genotypes or across ages, followed by Scheffe's *post hoc* test. The number of co-localized CaV1.3–RIBEYE puncta was significantly lower at P7 in *Pit1*^{dw} IHCs than in WT IHCs (P = 0.004), but not different at P14 (Fig. 2a–d and i). These data suggested that clustering of CaV1.3 at ribbon synapses was delayed at P7 in *Pit1*^{dw} IHCs but reached normal levels by P14. The number of CaV1.3 puncta at P14 was, however, significantly higher in *Pit1*^{dw} IHCs than in WT IHCs (P = 2.2E-9) (Fig. 2c, d and h). We inferred from these data that the excess ribbon synapses seen at P14 in *Pit1*^{dw} mice were not coupled with CaV1.3, and therefore may be functionally inactive. At P24, however, most of the RIBEYE puncta were juxtaposed with CaV1.3 puncta in *Pit1*^{dw} IHCs, and, interestingly, there were significantly higher (P = 0.01) numbers of these functional synaptic puncta in *Pit1*^{dw} IHCs than in control IHCs at this age (Fig. 2e, f and i). We also examined the changes in expression for these markers across the three ages tested (P7, P14, and P24) within a given genotype (WT or *Pit1*^{dw} mice) to determine the developmental time course for the formation of mature ribbon synapses that contain CaV1.3. WT IHCs had counts for CaV1.3 and co-localized RIBEYE–CaV1.3 puncta that were comparable at P14 and P24 (P = 0.15) but significantly lower than the respective values at P7 (P = 3.3E-10 for P14 vs. P7; P = 4.6E-10 for P24 vs. P7), indicating that functional synapses had undergone refinement in WT mice by P14 (Fig. 2h and i). In *Pit1*^{dw} mice, however, CaV1.3 counts at P7 and P14 were comparable, whereas those at P24 were significantly lower than at either of these ages (P = 1.5E-9 and P = 6.5E-9 for P24 vs. P7 and P24 vs. P14, respectively) (Fig. 2h). Interestingly, the numbers of colocalized RIBEYE–CaV1.3 puncta at P14 in *Pit1*^{dw} mice were significantly lower than those at both P7 and P24 (P = 0.001 for both comparisons) (Fig. 2i).

To examine whether the presence of excess synapses or the immature synaptic properties of *Pit1*^{dw} IHCs affected their function, we measured calcium currents and vesicle fusion changes in *Pit1*^{dw} and WT IHCs at various time points during development (between P2 and P24). In these experiments, calcium currents from both *Pit1*^{dw} and WT IHCs matured at different ages during the first postnatal week (Beutner & Moser, 2001; Johnson *et al*., 2005). The calcium current was high initially in WT IHCs, but plateaued from P7 onwards (one-way ANOVA with current measurement as the dependent variable and age as the independent factor followed by Scheffe's *post-hoc* tests showed that calcium currents at P7, P14 and P24 were comparable to each other, but were all significantly lower than the calcium current at P4: P = 5.2E-5 for P4 vs. P7; P = 0.002 for P4 vs. P14; P = 2.3E-7 for P4 vs. P24) (Marcotti *et al*., 2003). In *Pit1*^{dw} IHCs, however, the calcium current was still high at P7, and maturation was delayed (Fig. 3c). It eventually matured by P14 in *Pit1*^{dw} IHCs (a similar one-way ANOVA for calcium current data from *Pit1*^{dw} IHCs, followed by Scheffe's *post hoc* tests, showed that calcium currents at P14 and P21 were not significantly different from each

other, but were both lower than the calcium current at P7: $P = 0.017$ for P7 vs. P14; $P = 0.013$ for P7 vs. P24) (Fig. 3a–c). The calcium current at P14 in *Pit1*^{dw} IHCs was comparable to the calcium current in WT IHCs. No significant differences were observed in the voltage of half-activation during development for either the WT or the *Pit1*^{dw} mice (data not shown). Taken together, these data suggest that TH is required for the normal clustering and/ or pruning of CaV1.3 during development, similarly to what we observed with RIBEYE (Fig. 1a and b). Our electrophysiology measurements showed that, after an initial delay in maturation, there were normal calcium currents at P14 and at P24 in *Pit1*^{dw} IHCs. The excess number of CaV1.3 puncta and functional synapses at these ages did not correlate with the measured calcium current amplitude, suggesting that the number of channels per puncta was reduced or perhaps that single-channel conductance was altered during normal hair cell maturation, as previously described (Zampini *et al*., 2010).

Two sine capacitance measurements in Pit1 and WT IHCs—Both vesicle trafficking and vesicle fusion are triggered by calcium influx through CaV1.3 calcium channels (Beutner & Moser, 2001; Brandt *et al*., 2003, 2005; Fuchs *et al*., 2003; Moser *et al*., 2006). A change in the calcium channel distribution is predicted to alter synaptic release properties. Therefore, we investigated whether the initial delay in CaV1.3 current maturation in *Pit1*^{dw} IHCs mice altered neurotransmitter release during development. We used two sine capacitance measurements that allowed us to monitor capacitance continually during a depolarization (Schnee *et al*., 2011). Previous work identified two components of release, i.e. an initial fast component that saturated quickly and correlated with vesicles immediately near to the synapse, and a second, larger component of release, termed superlinear, that required recruitment of additional vesicles. Using this method, we found that the initial delay in calcium current maturation during the early postnatal period (P2 and P7) did not affect total vesicle release in *Pit1*^{dw} IHCs as compared with WT IHCs (Fig. 4a, b and d). At P14, however, despite similar calcium current measurements in both *Pit1*^{dw} and WT IHCs, capacitance measurements showed normal first-component release (release at 200 ms) (Fig. 4c) but lower total vesicle release (Fig. 4d), suggesting reduced vesicle replenishment or second-component release in *Pit1*^{dw} IHCs as compared with WT IHCs. At P24, total vesicle release reached nearly normal levels in *Pit1*^{dw} IHCs (Fig. 4d), indicating that the reduced vesicle replenishment phenotype seen at P14 in these mice was likely to be the result of a developmental delay.

Our study revealed that the absence of TH during the early postnatal period of cochlear neuronal development caused a delay in the pruning and clustering of presynaptic elements important for the function of afferent IHC synapses. Despite the excess number of synapses in these hypothyroid IHCs, the number of functional synapses reached normal levels by the age of onset of hearing (P14). This subset of structurally and functionally mature synapses was sufficient to drive a normal calcium current and first-component vesicle release at P14 and P24. The higher number of functional synapses at P24 in *Pit1*^{dw} IHCs indicates that calcium current and vesicle release per synapse were perhaps reduced as compared with WT synapses, resulting in comparable calcium current and capacitance. We next examined whether TH replacement would restore normal synaptic pruning in the afferent synapses of *Pit1*^{dw} IHCs.

TH replacement rescues normal synaptic pruning in *Pit1*^{dw} IHCs

We injected *Pit1*^{dw} mice with TH for specific time windows during the early postnatal period (Fig. 5h). These time windows were initially chosen on the basis of reports of higher deiodinase 2 activity and TH transporter levels in the cochlea from P5 to P8 suggesting that a greater amount of the active T3 form of TH was available at this period (Campos-Barros *et al*., 2000; Sharlin *et al*., 2011). We hypothesized that, if TH were required for pruning in this time window, supplementing with TH during this period would rescue the abnormal synaptic pruning phenotype that we saw in the *Pit1*^{dw} mice (Fig. 1). We examined the synapses in the IHCs of TH-treated Pit1^{dw} mice by immunohistochemistry. Our initial studies with TH replacement in two distinct time windows (from P5 to P8, and from P4 to P8) did not show significant differences between the treated and untreated groups at P14, with respect to number of puncta labelled with RIBEYE and SHANK1 (Fig. 5c, d and h). We then extended the duration of TH replacement from P3 to P8. Confocal images of cochlear whole mounts stained with antibodies against RIBEYE and SHANK1 are shown from the mid-turn for salineinjected WT and TH-treated *Pit1*^{dw} mice at P14 in Fig. 5a and b. We quantified the marker (RIBEYE, SHANK1 and RIBEYE–SHANK1) puncta, and then performed one-way ANOVA with marker count as the dependent variable and treatment group as the independent factor ($F_{2,12}$ = 28.429, P = 0.001 for RIBEYE; $F_{2,12}$ = 65.263, P = 0.001for SHANK1; $F_{2,12}$ = 35.686, P = 0.008 for RIBEYE–SHANK1). RIBEYE, SHANK1 and RIBEYE–SHANK1 counts in IHCs of TH-treated *Pit1*^{dw} mice (Fig. 5b and e) were similar to those in saline-treated WT mice at P14 (Fig. 5a and e). Also, as expected, RIBEYE, SHANK1 and RIBEYE–SHANK1 marker counts were significantly lower in IHCs of TH-treated *Pit1*^{dw} mice than in those of saline-treated *Pit1*^{dw} mice (P = 5E-5 for RIBEYE; P = 1E-6 for SHANK1; P = 1.7E-5 for RIBEYE–SHANK1; Scheffe's *post hoc* test). Treatment with TH from P3 to P8 restored a normal synaptic pattern and a normal number in *Pit1*^{dw} mice, as indicated by the results described above. We then investigated whether TH-mediated pruning can be completed before P8 by supplementing with TH from P3 to P4 (Fig. 5f) and from P3 to P6 (Fig. 5g). For the P3 to P4 window, RIBEYE, SHANK1 and RIBEYE–SHANK1 marker counts in *Pit1*^{dw} mice treated with TH were similar to those in saline-treated *Pit1*^{dw} mice (Fig. 5f). This result indicated that TH treatment from P3 to P4 was insufficient to restore normal pruning in these mice. Treatment of *Pit1*^{dw} mice with TH from of P3 to P6 resulted in a significant reduction in the numbers of both RIBEYE (P = 0.002) and RIBEYE–SHANK1 (P = 0.006) puncta, but not of SHANK1 puncta, as compared with saline-treated *Pit1*^{dw} mice (Fig. 5g). Likewise, counts for RIBEYE and RIBEYE-SHANK1 puncta were comparable to those in WT mice, but that for SHANK1 was still significantly higher than in WT mice in the P3 to P6 treatment group (P = 0.001). Therefore, we inferred that the window from P6 to P8 might be required to complete postsynaptic pruning. The different TH treatment windows and percentages of presynaptic and postsynaptic pruning with respect to pruning in WT mice are summarized in Fig. 5h. Additionally, we considered two more TH treatment windows, i.e. from P0 to P5 and from P5 to P10, to rule out the possibility that any 5-day period of TH supplementation during the early postnatal days would produce the same benefits as the P3 to P8 treatment. Quantification of RIBEYE and SHANK1 puncta from the cochleas of *Pit1*^{dw} mice treated from P0 to P5 or from P5 to P10 did not show normal synaptic pruning as seen with the P3 to P8 treatment (data not shown). In addition to RIBEYE and SHANK1, we also

investigated whether TH supplementation would restore the normal CaV1.3 distribution in *Pit1*^{dw} mice, but found no changes in this regard with TH treatment from P3 to P8 (data not shown). Perhaps more prolonged or even permanent TH supplementation may be necessary to establish normal CaV1.3 clustering, such as that performed by Sendin *et al*. (2007). Taken together, these results showed that the critical critical time window for TH action on afferent synaptic pruning in the cochlea was from P3 to P8. These findings constitute the first direct demonstration of TH rescuing a synaptic pruning defect in TH-deficient animals. We next investigated whether TH is important for the long-term maintenance of afferent synapses.

Homeostatic maintenance of afferent synapses is disrupted in young adult *Pit*^{dw}mice

Reduced afferent postsynaptic puncta in hypothyroid IHCs with age—Spiral ganglion neurons are target cells of TH in the developing and adult cochlea. The observation that the TH receptor α-subunit continues to be expressed in adult spiral ganglion neurons suggests a more sustained role for TH in the ear (Lautermann & ten Cate, 1997). We next examined whether, in addition to its role in synaptic development and pruning, TH was also involved in the homeostatic maintenance of healthy synapses over a long-term period, such as during aging. We examined WT and *Pit1*^{dw} IHCs by using immuno-histochemistry with RIBEYE and SHANK1 on whole mount preparations of the organ of Corti from mice at P42 (Fig. 6a–c; only midturn shown). At P42, the total numbers of RIBEYE puncta per IHC dw those in saline-treated WT mice at P14 (Fig. 5a and e). Also, as were comparable in *Pit1*^{dw} and WT IHCs ($P = 0.61$, Student's *t*-test) (Fig. 6c). However, the number of postsynaptic SHANK1 and RIBEYE–SHANK1 puncta at P42 were significantly reduced in *Pit1*^{dw} IHCs as compared with WT IHCs (SHANK1, $P = 0.001$; synapses, $P = 0.002$; Student's *t*-test). Taken together, these obser-vations suggested degeneration of afferent terminals at the base of *Pit1*^{dw} IHCs with age.

Degeneration of afferent terminals at the base of the IHCs in Pit^{dw} mice—We used TEM to further examine the potential degeneration of afferent terminals at the base of *Pit1*^{dw} IHCs and compared them with WT IHCs. We observed swollen afferent dendrites filled with vacuoles at P21 and P42 in Pit1^{dw} IHCs but not in WT IHCs (Fig. 7a and b; only P42 data shown). This novel feature suggested synaptic damage in the form of excitotoxicity to the afferent dendritic region of *Pit1*^{dw} IHCs, which has, so far, never been reported in any hypothyroid animal model. A similar pattern of dendritic damage was also seen in guinea pigs treated with the glutamate receptor agonist AMPA, and in mice lacking the glutamate transporter GLAST (Puel *et al*., 1991; Hakuba *et al*., 2000). Given that the glial high-affinity glutamate transporters GLT-1 and GLAST are encoded by TH-regulated genes (Mendes-de-Aguiar *et al*., 2008; Zamoner *et al*., 2008), we hypothesized that lower GLAST levels in the supporting cells surrounding the IHCs in hypothyroid animals might lead to less glutamate being cleared from the synaptic cleft. This buildup of glutamate, over a period of time, could result in excitotoxic damage to the afferent dendrites connected to IHCs, as observed in the TEM images above (Fig. 7a and b).

To examine whether the buildup of glutamate at the synaptic cleft could cause damage to the afferent terminals in *Pit1*^{dw} mice, we checked the transcript and protein levels of GLAST by quantitative RT-PCR and immunofluorescence staining. We found no significant differences

in the levels of GLAST mRNA in the organ of Corti of *Pit1*^{dw} vs. WT mice at P9 and P12 (data not shown). We then examined the protein expression of GLAST by immunohistochemistry at P14 on whole mount cochlear tissue. The IHCs were marked with an anti-myosin VIIa antibody in WT and *Pit*^{dw} mice (Fig. 7c and d). We saw a substantial reduction in GLAST staining along the plasma membrane of the inner phalangeal cells in *Pit*^{dw} cochlea as compared with WT controls (Fig. 7e and f). We next investigated whether normal levels of GLAST protein expression could be restored in *Pit*^{dw} mice treated with TH. TH treatment from P3 to P8 at least partially restored GLAST expression in the inner phalangeal cells of *Pit*^{dw} mice at P14 as compared with saline-treated WT mice (Fig. 7g and h). Together, these data suggested an important role for TH in the homeostatic maintenance of healthy synapses by regulating GLAST expression post-transcriptionally.

Discussion

This study represents a comprehensive analysis concerning the effect of TH deficiency on the functional maturation and maintenance of IHC afferent synapses. We observed abnormal persistence of excess afferent synaptic connectivity in the absence of TH. We found that only a subset of excess synapses in *Pit1*^{dw} mice were structurally and functionally mature, but this group was sufficient to drive normal calcium currents and vesicle release by adulthood. We restored synaptic pruning in *Pit1*^{dw} IHCs by TH replacement from P3 to P8, establishing this window as being critical for the effect of TH on this process. Finally, we discovered a new role for TH in the homeostatic maintenance of IHC afferent terminals as they age, via regulation of GLAST protein levels.

Critical window of TH action on IHC afferent synaptic pruning

Defective cochlear afferent fibre retraction and abnormal persistence of multi-ribbon formation at the active zone in outer hair cells and IHCs, respectively, have been reported in different hypothyroid models (Uziel *et al*., 1983; Sendin *et al*., 2007). Our present study suggests that the last stage of afferent neurite development when excess connections undergo extensive pruning and retained synapses mature functionally was impaired in the absence of TH.

Synaptic pruning takes place after the peak of synapse formation that occurs at around P4 in rodents (Sobkowicz *et al*., 1982; Huang *et al*., 2012; Wong *et al*., 2014). We observed significantly higher numbers of synapses at P9 and P14 in *Pit1*^{dw} IHCs than in WT IHCs, suggesting defective pruning in hypothyroid IHCs. It has been reported that the activity of the enzyme deiodinase 2, which converts TH from T4 to the more active T3 form, peaks from P5 to P8 in the rodent cochlea (Campos-Barros *et al*., 2000). This increase in deiodinase 2 activity also coincides with high expression levels of TH transporters in the cochlea (Sharlin *et al*., 2011; Ng *et al*., 2013). These observations suggest that TH is most active in the cochlea during this period. However, injecting *Pit1*^{dw} mice with TH from P3 to P8, rather than from P3 to P4, from P4 to P8, or from P5 to P8, was most effective in rescuing the synapse-pruning defect in these mice, indicating that the earlier time point is critical for TH action on this process. P3 to P6 treatment was almost as effective as P3 to P8 treatment for presynaptic pruning, but postsynaptic pruning was not completed by P6. This

result indicates that TH action was required up to P8 for completion of postsynaptic pruning. It also suggests that presynaptic pruning may precede postsynaptic disassembly.

Further evidence to support this idea comes from our observation of partial pruning of only the presynaptic ribbons in *Pit1*^{dw} mice at later ages during the refinement period. This result indicates that presynaptic pruning occurs to at least some extent in these mice, even when there is no pruning postsynaptically. Partial presynaptic pruning in *Pit1*^{dw} IHCs could be attributable to the involvement of a cofactor that acts synergistically with TH to mediate pruning, or could perhaps occur because TH modulates the rate of existing mechanisms and its absence merely delays these processes.

Afferent synaptic activity in hypothyroid IHCs

In both the developing central and peripheral nervous systems, synaptic activity-dependent and synaptic activity-independent mechanisms have been implicated in synapse formation and pruning (Verhage, 2000; Cohen-Cory, 2002; Molnar & Isaac, 2002; Goda & Davis, 2003). Mechanisms underlying these processes in the cochlea are poorly understood; however, it is well known that the initiation of synaptic activity precedes the completion of synapse formation and pruning (Beutner & Moser, 2001; Johnson *et al*., 2013). Interestingly, synapse formation and pruning do not seem to depend on the synaptic activity of the IHCs, as suggested by studies in mice deficient for CaV1.3 and otoferlin (Nemzou *et al*., 2006; Roux *et al*., 2006). In addition, mice lacking a functional bassoon protein also show generally intact calcium-dependent exocytosis activity, even though ribbon formation was disrupted in these mice (Jing *et al*., 2013). These studies suggest that synaptic activity of IHCs may be independent of synapse formation and pruning processes and vice versa. In *Pit1*^{dw} mice, our electrophysiological data showed that, despite an initial delay, the normal developmental maturation/ reduction of the maximum calcium current amplitude had taken place in the absence of TH by the age of onset of hearing. Our results are, in some ways, similar to previous reports indicating a developmental delay in synaptic functional maturation in the absence of TH (Brandt *et al*., 2007; Sendin *et al*., 2007). The difference, however, is that whereas they reported that calcium currents remained abnormally elevated near the level of the immature maximum peak current in their hypothyroid models, we found recovery to normal levels in *Pit1*^{dw} mice by the age of onset of hearing. These differences in observations can perhaps be attributed to the diversity in the genetic backgrounds of the hypothyroid models studied. With respect to capacitance measurements, we found that the first component of release was unaffected in *Pit1*^{dw} IHCs throughout development and up to P24. However, total release data suggested a delay in vesicle replenishment at P14, despite the normal calcium current. When correlated with morphological data, our immunohistochemistry study revealed that the excess synaptic (RIBEYE–SHANK1) puncta in hypothyroid IHCs might not represent ‘functional’ synapses, owing to the absence of co-localized CaV1.3 puncta in them. The subset of functional synapses in *Pit1*^{dw} IHCs, however, appear to be sufficient to generate normal calcium currents and a normal first component of release from the age of onset of hearing and also in the young adults. The increased number of functional synapses seen at P24 in *Pit1*^{dw} IHCs may reflect an attempt to compensate for the deficit in vesicle replenishment seen at P14 in *Pit1*^{dw} IHCs.

On the basis of these data, we propose that TH is required for elimination of the excess synapses formed during development and for triggering mechanisms involved in the development of the initial calcium current, but not for the later stages of functional maturation in these cells.

Homeostatic maintenance of afferent synapses in young adult Pit1^{dw} mice

In addition to the immediate effects of TH on synapse pruning in the early postnatal period, the effects of TH and/or other factors on the long-term maintenance of mature synapses are also of interest to our group (Mendus *et al*., 2014). One group of genes that are TH-regulated and are crucial for synapse maintenance are those encoding the glial glutamate transporters GLAST and GLT-1 (Mendes-de-Aguiar *et al*., 2008; Zamoner *et al*., 2008). In this study, we have shown, for the first time, that the expression level of GLAST protein (but not mRNA) in the organ of Corti is TH-dependent. This result suggests that TH may regulate GLAST expression at the post-transcriptional stage, such as in the trafficking of the protein to cell membranes. GLAST is the only glutamate transporter detected in the organ of Corti, and is responsible for transmitter uptake at IHC afferent synapses (Li *et al*., 1994; Rebillard *et al*., 2003; Glowatzki *et al*., 2006). Reduction of GLAST expression in supporting cells could explain the glutamate excitotoxicity phenotype of the afferent nerve endings in *Pit1*^{dw} mice at later ages. Similar afferent terminal damage was seen in noise-exposed GLAST- deficient mice (Hakuba *et al*., 2000). In addition, excitotoxicity resulting from extracellular glutamate buildup was shown in the brains of hypothyroid rats, and was linked to reduced GLAST levels, supporting the idea that similar mechanisms may operate in the hypothyroid cochlea (Cattani *et al*., 2013). A cartoon summarizing these observations with respect to synaptic pruning and maintenance in WT and hypothyroid IHCs is given in Fig. 8.

The next set of experiments will be directed towards defining the cell types and the network of TH-regulated genes that drive afferent synaptic pruning, maturation, and maintenance. Recent studies from our laboratory and others have provided further support for the growing evidence in favour of a major role for the supporting cells and the spiral ganglion neurons in cochlear synapse formation and maturation (Tritsch *et al*., 2007; Wan *et al*., 2013; Mendus *et al*., 2014; Yu & Goodrich, 2014). Developing a mouse model with cellspecific TH deficiency can be a valuable tool to help identify candidate regulatory factors expressed in the different cochlear cell types. The relevant mouse models for these candidates can then be studied to answer unresolved questions in the field, such as whether the persistence of transient synapses would affect normal hearing during development.

Acknowledgements

This work was supported by research and core grants from the National Institute in Deafness and other Communicative Disorders: R01 DC09590 (M. Mustapha), R01 DC009913 (A. Ricci), and P30 DC010363 (S. Heller, Stanford University). We thank Lars Becker for help with computer-related issues and the schematic cartoon. We also acknowledge support from Dr Sally Camper and the March of Dimes Foundation during the initial phase of this work. The authors sincerely thank Dr Srikantan Nagarajan for advice on statistics, and Dr Sally Camper for helpful comments and critical discussions throughout the duration of this study. The authors declare no competing financial interests.

Abbreviations

IHC	inner hair cell
P	postnatal day
PBS	phosphate-buffered saline
RT-PCR	reverse transcription-polymerase chain reaction
T3	3,5,3′-triiodothyronine sodium salt
T4	thyroxine
TEM	transmission electron microscopy
TH	thyroid hormone
WT	wild-type

References

Bernal J. Thyroid hormones and brain development. Vitam. Horm. 2005; 71:95–122. [PubMed: 16112266]

Beutner D, Moser T. The presynaptic function of mouse cochlear inner hair cells during development of hearing. J. Neurosci. 2001; 21:4593–4599. [PubMed: 11425887]

Brandt A, Striessnig J, Moser T. CaV1.3 channels are essential for development and presynaptic activity of cochlear inner hair cells. J. Neurosci. 2003; 23:10832–10840. [PubMed: 14645476]

Brandt A, Khimich D, Moser T. Few CaV1.3 channels regulate the exocytosis of a synaptic vesicle at the hair cell ribbon synapse. J. Neurosci. 2005; 25:11577–11585. [PubMed: 16354915]

Brandt N, Kuhn S, Münkner S, Braig C, Winter H, Blin N, Engel J. Thyroid hormone deficiency affects postnatal spiking activity and expression of Ca^{2+} and K^{+} channels in rodent inner hair cells. J. Neurosci. 2007; 27:3174–3186. [PubMed: 17376979]

Campos-Barros A, Amma LL, Faris JS, Shailam R, Kelley MW, Forrest D. Type 2 iodothyronine deiodinase expression in the cochlea before the onset of hearing. Proc. Natl. Acad. Sci. USA. 2000; 97:1287–1292. [PubMed: 10655523]

Cattani D, Goulart PB, Cavalli VLDLO, Winkelmann-Duarte E, Dos Santos AQ, Pierozan P, Zamoner A. Congenital hypothyroidism alters the oxidative status, enzyme activities and morphological parameters in the hippocampus of developing rats. Mol. Cell. Endocrinol. 2013; 375:14–26. [PubMed: 23693027]

Cohen-Cory S. The developing synapse: construction and modulation of synaptic structures and circuits. Science (New York). 2002; 298:770–776.

Deol MS. Congenital deafness and hypothyroidism. Lancet. 1973; 2:105–106. [PubMed: 4123609]

Ehret G. Development of absolute auditory threshold in the house mouse (Mus musculus). J. Am. Audiol. Soc. 1976; 1:179–184. [PubMed: 956003]

Engel J, Michna M, Platzer J, Striessnig J. Calcium channels in mouse hair cells: function, properties and pharmacology. Adv. Otorhinolaryng. 2002; 59:35–41.

Fuchs PA, Glowatzki E, Moser T. The afferent synapse of cochlear hair cells. Curr. Opin. Neurobiol. 2003; 13:452–458. [PubMed: 12965293]

Glowatzki E, Cheng N, Hiel H, Yi E, Tanaka K, Ellis-Davies GCR, Bergles DE. The glutamate–aspartate transporter GLAST mediates glutamate uptake at inner hair cell afferent synapses in the mammalian cochlea. J. Neurosci. 2006; 26:7659–7664. [PubMed: 16855093]

Goda Y, Davis GW. Mechanisms of synapse assembly and disassembly. Neuron. 2003; 40:243–264. [PubMed: 14556707]

Hakuba N, Koga K, Gyo K, Usami SI, Tanaka K. Exacerbation of noise-induced hearing loss in mice lacking the glutamate transporter GLAST. J. Neurosci. 2000; 20:8750–8753. [PubMed: 11102482]

Huang LC, Thorne PR, Housley GD, Montgomery JM. Spatiotemporal definition of neurite outgrowth, refinement and retraction in the developing mouse cochlea. Development. 2007; 134:2925–2933. [PubMed: 17626062]

Huang L-C, Barclay M, Lee K, Peter S, Housley GD, Thorne PR, Montgomery JM. Synaptic profiles during neurite extension, refinement and retraction in the developing cochlea. Neural Dev. 2012; 7:38. [PubMed: 23217150]

Jing Z, Rutherford MA, Takago H, Frank T, Fejtova A, Khimich D, Strenzke N. Disruption of the presynaptic cytomatrix protein bassoon degrades ribbon anchorage, multiquantal release, and sound encoding at the hair cell afferent synapse. J. Neurosci. 2013; 33:4456–4467. [PubMed: 23467361]

Johnson SL, Marcotti W, Kros CJ. Increase in efficiency and reduction in Ca^{2+} dependence of exocytosis during development of mouse inner hair cells. J. Physiol. 2005; 563(Pt 1):177–191. [PubMed: 15613377]

Johnson SL, Kuhn S, Franz C, Ingham N, Furness DN, Knipper M, Marcotti W. Presynaptic maturation in auditory hair cells requires a critical period of sensory-independent spiking activity. Proc. Natl. Acad. Sci. USA. 2013; 110:8720–8725. [PubMed: 23650376]

Karolyi IJ, Dootz GA, Halsey K, Beyer L, Probst FJ, Johnson KR, Camper SA. Dietary thyroid hormone replacement ameliorates hearing deficits in hypothyroid mice. Mamm. Genome. 2007; 18:596–608. [PubMed: 17899304]

Knipper M, Gestwa L, Ten Cate WJ, Lautermann J, Brugger H, Maier H, Zenner HP. Distinct thyroid hormone-dependent expression of TrKB and p75NGFR in nonneuronal cells during the critical TH-dependent period of the cochlea. J. Neurobiol. 1999; 38:338–356. [PubMed: 10022577]

Lautermann J, ten Cate WJ. Postnatal expression of the alphathyroid hormone receptor in the rat cochlea. Hear. Res. 1997; 107:23–28. [PubMed: 9165343]

Li H-S, Niedzielski AS, Beisel KW, Hiel H, Wenthold RJ, Morley BJ. Identification of a glutamate/aspartate transporter in the rat cochlea. Hear. Res. 1994; 78:235–242. [PubMed: 7527019]

Marcotti W, Johnson SL, Holley MC, Kros CJ. Developmental changes in the expression of potassium currents of embryonic, neonatal and mature mouse inner hair cells. J. Physiol. 2003; 548(Pt 2): 383–400. [PubMed: 12588897]

Mendes-de-Aguiar CB, Alchini R, Decker H, Alvarez-Silva M, Tasca CI, Trentin AG. Thyroid hormone increases astrocytic glutamate uptake and protects astrocytes and neurons against glutamate toxicity. J. Neurosci. Res. 2008; 86:3117–3125. [PubMed: 18543341]

Mendus D, Sundaresan S, Grillet N, Wangsawihardja F, Leu R, Müller U, Mustapha M. Thrombospondins 1 and 2 are important for afferent synapse formation and function in the inner ear. Eur. J. Neurosci. 2014; 39:1256–1267. [PubMed: 24460873]

Michna M, Knirsch M, Hoda J-C, Muenkner S, Langer P, Platzer J, Engel J. Cav1.3 (alpha1D) Ca^{2+} currents in neonatal outer hair cells of mice. J. Physiol. 2003; 553(Pt 3):747–758. [PubMed: 14514878]

Molnar E, Isaac JTR. Developmental and activity dependent regulation of ionotropic glutamate receptors at synapses. Scientific World J. 2002; 2:27–47.

Moser T, Brandt A, Lysakowski A. Hair cell ribbon synapses. Cell Tissue Res. 2006; 326:347–359. [PubMed: 16944206]

Mustapha M, Fang Q, Gong TW, Dolan DF, Raphael Y, Camper SA, Duncan RK. Deafness and permanently reduced potassium channel gene expression and function in hypothyroid Pit1dw mutants. J. Neurosci. 2009; 29:1212–1223. [PubMed: 19176829]

Nemzou NR, Bulankina AV, Khimich D, Giese A, Moser T. Synaptic organization in cochlear inner hair cells deficient for the CaV1.3 (alpha1D) subunit of L-type Ca^{2+} channels. Neuroscience. 2006; 141:1849–1860. [PubMed: 16828974]

Ng L, Kelley MW, Forrest D. Making sense with thyroid hormone – the role of T(3) in auditory development. Nat. Rev. Endocrinol. 2013; 9:296–307. [PubMed: 23529044]

Paolicelli RC, Bolasco G, Pagani F, Maggi L, Scianni M, Panzanelli P, Gross CT. Synaptic pruning by microglia is necessary for normal brain development. Science (New York). 2011; 333:1456–1458.

Peng AW, Effertz T, Ricci AJ. Adaptation of mammalian auditory hair cell mechanotransduction is independent of calcium entry. Neuron. 2013; 80:960–972. [PubMed: 24267652]

Puel J-L, Pujol R, Ladrech S, Eybalin M. Alpha-amino-3-hydroxy-5-methyl-4-isoxazole proionic acid electrophysiological and neurotoxic effects in the guinea-pig cochlea. Neuroscience. 1991; 45:63–72. [PubMed: 1684414]

Rebillard G, Ruel J, Nouvian R, Saleh H, Pujol R, Dehnes Y, Devau G. Glutamate transporters in the guinea-pig cochlea: partial mRNA sequences, cellular expression and functional implications. Eur. J. Neurosci. 2003; 17:83–92. [PubMed: 12534971]

Roux I, Safieddine S, Nouvian R, Grati M, Simmler M-C, Bahloul A, Petit C. Otoferlin, defective in a human deafness form, is essential for exocytosis at the auditory ribbon synapse. Cell. 2006; 127:277–289. [PubMed: 17055430]

Rueda J, Prieto JJ, Cantos R, Sala ML, Merchan JA. Hypothyroidism prevents developmental neuronal loss during auditory organ development. Neurosci. Res. 2003; 45:401–408. [PubMed: 12657453]

Rusch A, Ng L, Goodyear R, Oliver D, Lisoukov I, Vennstrom B, Forrest D. Retardation of cochlear maturation and impaired hair cell function caused by deletion of all known thyroid hormone receptors. J. Neurosci. 2001; 21:9792–9800. [PubMed: 11739587]

Santos-Sacchi J. Determination of cell capacitance using the exact empirical solution of partial differential Y/partial differential Cm and its phase angle. Biophys J. 2004; 87:714–727. [PubMed: 15240504]

Santos-Sacchi J, Kakehata S, Takahashi S. Effects of membrane potential on the voltage dependence of motility-related charge in outer hair cells of the guinea-pig. J. Physiol. 1998; 510(Pt 1):225–235. [PubMed: 9625879]

Schnee ME, Kong J, Santos-sacchi J, Ricci AJ. Tracking vesicle fusion from hair cell ribbon synapses using a high frequency, dual sine wave stimulus paradigm. Commun. Integr. Biol. 2011; 4:785–787. [PubMed: 22446556]

Sendin G, Bulankina AV, Riedel D, Moser T. Maturation of ribbon synapses in hair cells is driven by thyroid hormone. J. Neurosci. 2007; 27:3163–3173. [PubMed: 17376978]

Sharlin DS, Visser TJ, Forrest D. Developmental and cell-specific expression of thyroid hormone transporters in the mouse cochlea. Endocrinology. 2011; 152:5053–5064. [PubMed: 21878515]

Sobkowicz HM, Rose JE, Scott GE, Slapnick SM. Ribbon synapses in the developing intact and cultured organ of Corti in the mouse. J. Neurosci. 1982; 2:942–957. [PubMed: 7097321]

Sui L, Wang F, Li BM. Adult-onset hypothyroidism impairs paired-pulse facilitation and long-term potentiation of the rat dorsal hippocampo-medial prefrontal cortex pathway in vivo. Brain Res. 2006; 1096:53–60. [PubMed: 16725120]

Tritsch NX, Yi E, Gale JE, Glowatzki E, Bergles DE. The origin of spontaneous activity in the developing auditory system. Nature. 2007; 450:50–55. [PubMed: 17972875]

Uziel A. Periods of sensitivity to thyroid hormone during the development of the organ of Corti. Acta Otolaryngol. Suppl. 1986; 429:23–27. [PubMed: 3461670]

Uziel A, Pujol R, Legrand C, Legrand J. Cochlear synaptogenesis in the hypothyroid rat. Brain Res. 1983; 283:295–301. [PubMed: 6850354]

Verhage M. Synaptic assembly of the brain in the absence of neurotransmitter secretion. Science. 2000; 287:864–869. [PubMed: 10657302]

Wan G, Corfas G, Stone JS. Inner ear supporting cells: rethinking the silent majority. Semin. Cell Dev. Biol. 2013; 24:448–459. [PubMed: 23545368]

Weiss RE, Murata Y, Cua K, Hayashi Y, Seo H, Refetoff S. Thyroid hormone action on liver, heart, and energy expenditure in thyroid hormone receptor beta-deficient mice. Endocrinology. 1998; 139:4945–4952. [PubMed: 9832432]

Wong AB, Rutherford MA, Gabrielaitis M, Pangrsic T, Göttfert F, Frank T, Moser T. Developmental refinement of hair cell synapses tightens the coupling of $^{Ca2+}$ influx to exocytosis. EMBO J. 2014; 33:247–264. [PubMed: 24442635]

Yu W-M, Goodrich LV. Morphological and physiological development of auditory synapses. Hear. Res. 2014; 311:3–16. [PubMed: 24508369]

Zamoner A, Heimfarth L, Pessoa-Pureur R. Congenital hypothyroidism is associated with intermediate filament misregulation, glutamate transporters down-regulation and MAPK activation in developing rat brain. Neurotoxicology. 2008; 29:1092–1099. [PubMed: 18845185]

Zampini V, Johnson SL, Franz C, Lawrence ND, Münkner S, Engel J, Marcotti W. Elementary properties of CaV1.3 Ca(2+) channels expressed in mouse cochlear inner hair cells. J. Physiol. 2010; 588(Pt 1):187–199. [PubMed: 19917569]

Zhan Y, Paolicelli RC, Sforazzini F, Weinhard L, Bolasco G, Pagani F, Gross CT. Deficient neuron–microglia signaling results in impaired functional brain connectivity and social behavior. Nat. Neurosci. 2014; 17:400–406. [PubMed: 24487234]

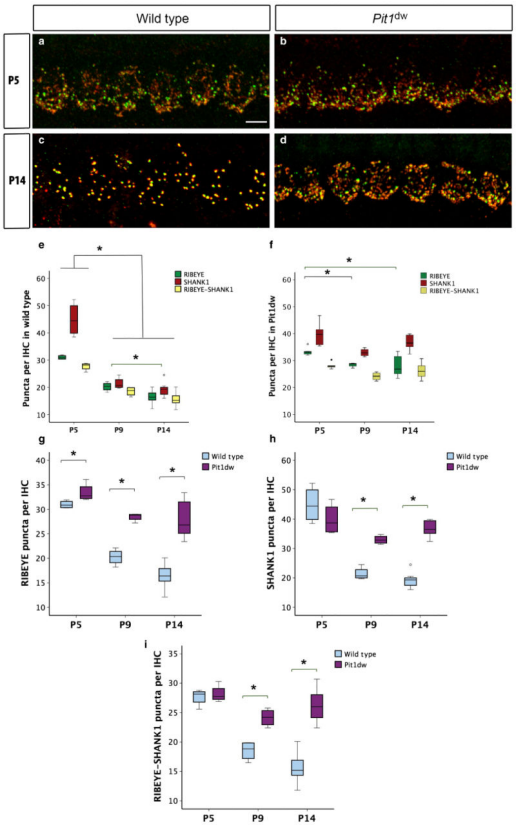

Fig. 1.

Synaptic pruning is disrupted in *Pit1*^{dw} IHCs. (a and b) Projection of confocal sections obtained from the mid-turn of cochlear whole mounts stained with afferent presynaptic (RIBEYE; green) and postsynaptic (SHANK1; red) markers at P5 in WT mice (a) and *Pit1*^{dw} mice (b). (c and d) The same markers at P14 in WT mice (c) and *Pit1*^{dw} mice (d). (e–i) Box plots of the quantification of RIBEYE, SHANK1 and RIBEYE–SHANK1 puncta from the mid-turn of the cochlea in WT and *Pit1*^{dw} mice. (e and f) RIBEYE, SHANK1 and RIBEYE–SHANK1 counts at P5, P9 and P14 in WT mice (e) and *Pit1*^{dw} mice (f). (g–i) Comparison of RIBEYE (g), SHANK1 (h) and RIBEYE–SHANK1 (i) counts between WT and *Pit1*^{dw} mice. significant comparisons ($P < 0.05$) are indicated with asterisks. The dots indicate outliers in the data.

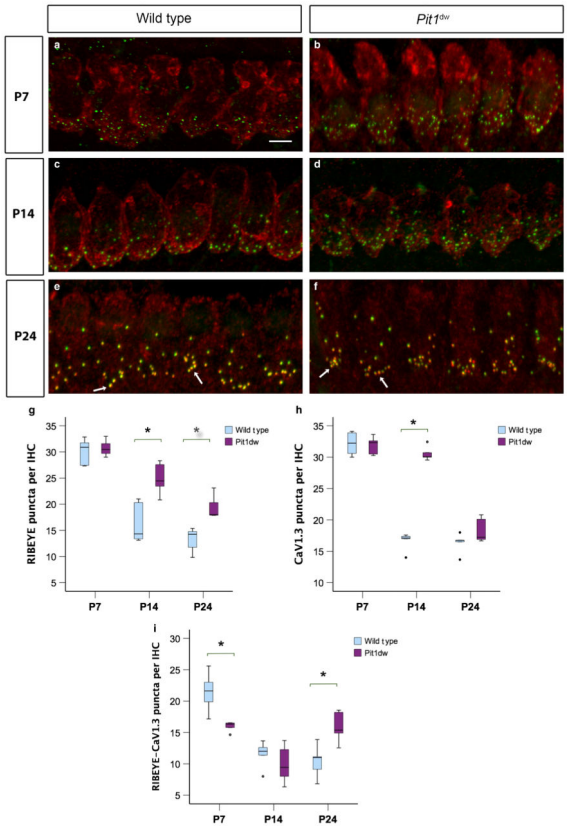

Fig. 2.

Abnormal CaV1.3 puncta clustering at the synapses of *Pit1*^{dw} IHCs. (a and b) Projection of confocal sections obtained from the mid-turn of cochlear whole mounts stained with the afferent presynaptic marker RIBEYE (green) and the calcium channel CaV1.3 (red) at P7 in WT mice (a) and *Pit1*^{dw} mice (b). (c–f) The same markers at P14 for WT (c) and *Pit1*^{dw} mice (d), and at P24 for WT (e) and *Pit1*^{dw} mice (f). (g–i) Box plots of the quantification of RIBEYE (g), CaV1.3 (h) and RIBEYE–CaV1.3 (i) puncta from the mid-turn of the cochlea in WT and *Pit1*^{dw} mice. significant comparisons ($P < 0.05$) between genotypes are indicated with asterisks. To maintain clarity of the figure, *P*-values for significant comparisons across different ages within the same genotype are not indicated on the graph, but are mentioned in the relevant Results section. The dots indicate outliers in the data.

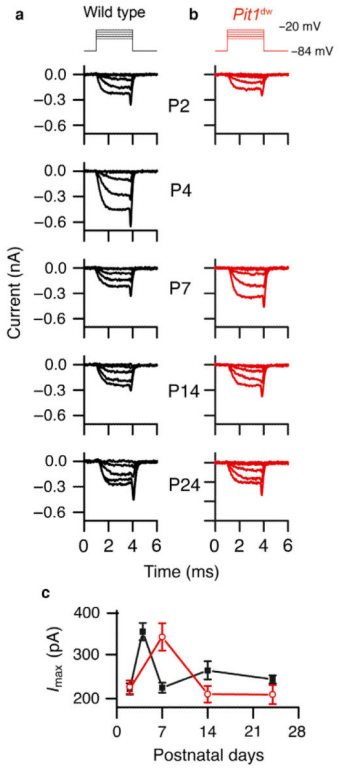

Fig. 3.

(a and b) Calcium current measurements from WT (a) and *Pit1*^{dw} (b) IHCs. The stimulus is shown at the top. Measurements were made at the ages indicated on the right. Hair cells were held at −84 mV and depolarized in 10-mV steps from −120 mV to +20 mV. The data shown include 20-mV steps from −80 mV to −60 mV. (c) Plots of the calcium current amplitudes at different postnatal days for WT (black) and *Pit1*^{dw} (red) IHCs. The number of WT and *Pit1*^{dw} IHCs recorded were, respectively, P2 (12 and 5), P4 (4 and 0), P7 (13 and 4), P14 (11 and 20), and P24 (9 and 12).

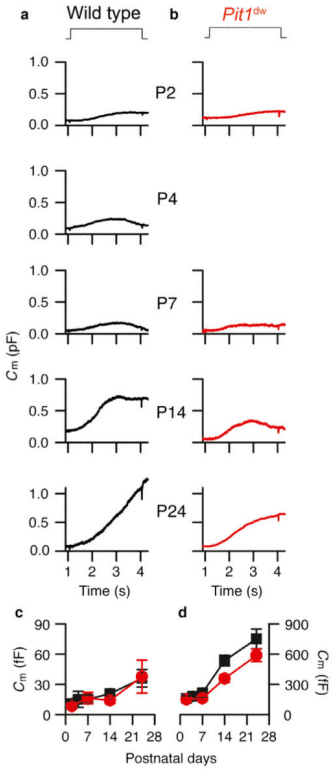

Fig. 4.

Two sine capacitance measurements from WT (a) and *Pit1*^{dw} (b) IHCs at different postnatal ages, as indicated. Capacitance was measured in response to a 3-s depolarization to −34 mV from a holding potential of −84 mV. The first component was measured at 200 ms into the step depolarization, and is summarized in (c), and full release is summarized in (d). The number of measurements were as follows for WT and *Pit1*^{dw} IHCs, respectively: P2 (6 and 4), P4 (2 and 0), P7 (4 and 3), P14 (6 and 5), and P24 (5 and 5).

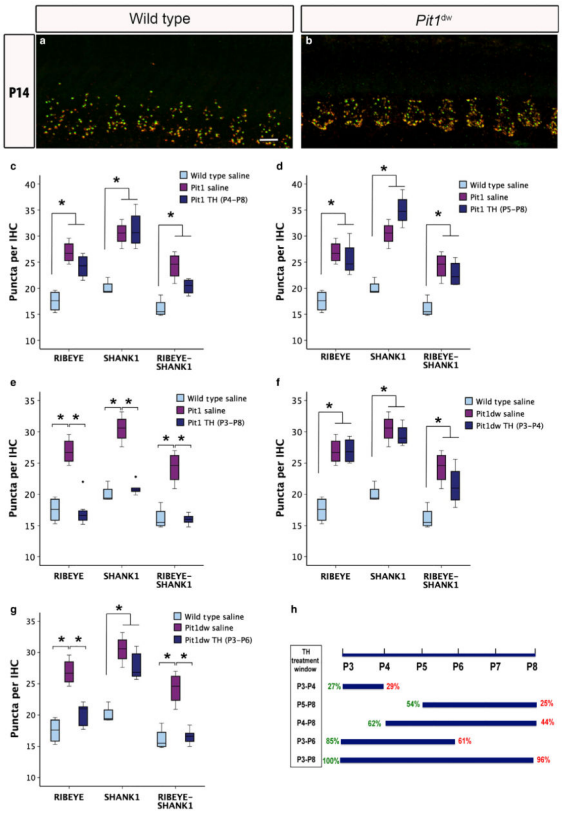

Fig. 5.

TH treatment from P3 to P8 restores normal synaptic counts in *Pit1*^{dw} IHCs. (a and b) Projection of confocal sections obtained from the mid-turn of cochlear whole mounts stained with RIBEYE (green) and SHANK1 (red) markers at P14 in saline-treated WT mice (a) and *Pit1*^{dw} mice (b) treated with TH from P3 to P8. Scale bar: 10 lm. (c–g) Box plots of the quantification of RIBEYE, SHANK1 and RIBEYE–SHANK1 puncta from the mid-turn of the cochlea in saline-treated WT and *Pit1*^{dw} mice, and in TH-treated *Pit1*^{dw} mice, for the following treatment windows: P4 to P8 (c), P5 to P8 (d), P3 to P8 (e), P3 to P4 (f), and P3 to P6 (g). significant comparisons ($P < 0.05$) are indicated with asterisks. The dots indicate outliers in the data. (h) Percentage of presynaptic (green) and postsynaptic (red) pruning for the different TH treatment groups with respect to WT controls. The duration of each treatment period is indicated with respect to the entire period examined from P3 to P8.

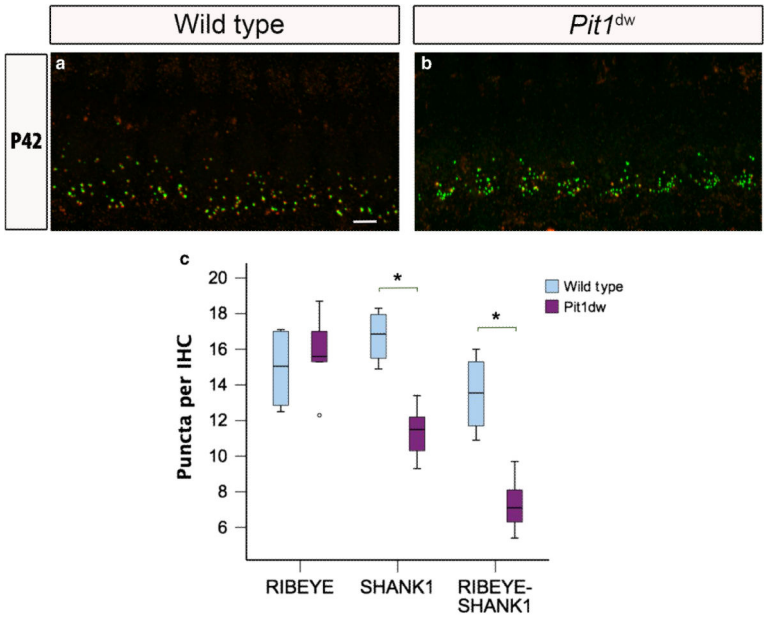

Fig. 6.

Reduced number of afferent postsynaptic counts in young adult *Pit1*^{dw} IHCs. (a and b) Projection of confocal sections obtained from the mid-turn of cochlear whole mounts stained with RIBEYE (green) and SHANK1 (red) markers in WT mice (a) and *Pit1*^{dw} mice (b) at P42. Scale bar: 10 lm. (c) Box plot of the quantification of RIBEYE, SHANK1 and RIBEYE–SHANK1 puncta from the mid-turn of WT and *Pit1*^{dw} cochlea at P42. significant comparisons ($P < 0.05$) are indicated with asterisks. The dots indicate outliers in the data.

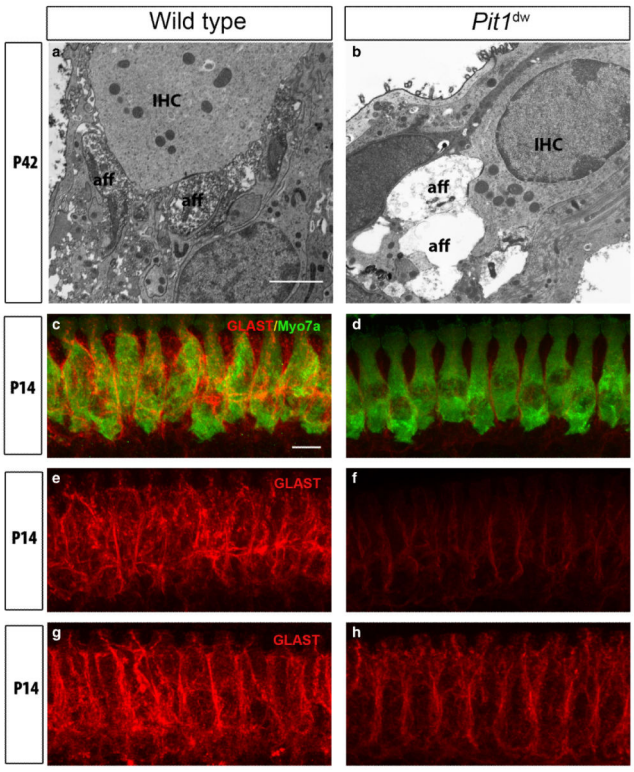

Fig. 7.

Swollen afferent type I terminals and reduced GLAST expression in young adult *Pit1*^{dw} mice. (a and b) Representative TEM images from the mid-turn of *Pit1*^{dw} and WT cochleas at P42. IHC and afferent boutons (aff) are indicated. Scale bar: 2 lm. (c and d) Projections of confocal sections obtained from the mid-turn of cochlear whole mounts co-stained with anti-GLAST (red) and anti-myosin VIIa (green) antibodies in WT and *Pit1*^{dw} mice at P14. (e and f) GLAST expression (red) alone in WT and *Pit1*^{dw} mice at P14 before TH treatment. (g and h) GLAST expression (red) at P14 in saline-treated WT mice and in TH-treated *Pit1*^{dw} mice from P3 to P8. Scale bar: 10 lm.

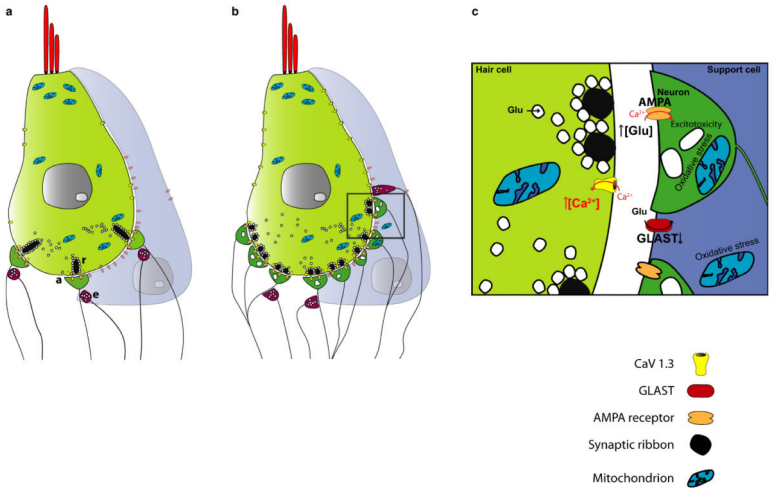

Fig. 8.

A cartoon representing normal and hypothyroid adult IHC synapses. (a) WT IHC. (b) Hypothyroid IHC. (c) Magnification of the box in b. A hypothyroid IHC is characterized by an excess of afferent synapses caused by the abnormal retention of afferent neurite branches and terminals, calcium channels being more widely distributed around the hair cell, and higher glutamate buildup at the synaptic cleft, owing to lower GLAST levels (b and c). In comparison, a normal IHC shows fewer but well-organized afferent terminals and a more clustered pattern of CaV1.3 calcium channel expression at the basal region of the hair cell. a, afferent fibre; e, efferent fibre; r, ribbon synapse.